AMORPHOUS SILICON FLAT PANEL IMAGERS FOR MEDICAL APPLICATIONS

A. Mireshghi

Sharif University of Technology
Tehran, Iran

T. Jing, S. N. Kaplan, H. K. Lee and V. Perez-Mendez

Lawrence Berkeley Laboratory
University of California
Berkeley, CA 94720, USA

Abstract A new gamma camera based on hydrogenated amorphous silicon (a-Si:H) pixel arrays to be used in nuclear medicine is introduced. Various performance characteristics of a-Si:H imagers are reviewed and compared with those of currently used equipment. An important component in the a-Si:H imager is the scintillator screen. A new approach for fabrication of high resolution CsI(Tl) scintillator layers, appropriate for coupling with a-Si:H arrays, are presented. Using Monte Carlo Simulation, the performance of the new a-Si:H based gamma camera is evaluated.

Key Words Amorphous Silicon, Flat Panel Imagers, Medical Imaging, Monte Carlo Simulation, Gamma Camera

چکیده در این مقاله، یک دوربین گامای جدید که براساس یک آرایه دوبعدی از سیلیکن بی شکل طراحی گردیده معرفی می شود. همچنین مشخصات و کارآیی تصویر گرهای جدید سیلیکن بی شکل با وسایل مشابه موجود در بازار مقایسه می گردد. یکی از بخشهای اساسی سیستم تصویرگر مورد نظر صفحه سوسوزن می باشد. در دوربین گامای معرفی شده ماده سوسوزن CsI (TI) که مشخصه تابش آن با منحنی حساسیت تصویرگر سیلیکن بی شکل انطباق خوبی دارد مورد استفاده قرار گرفته است. این ماده به صورت یک لایه با ساختار ستونی بهینه شده به روشی ابتکاری پوشش داده شده است. ساختار مزبور حد تفکیک مکانی را به نحو قابل ملاحظه ای بهبود بخشیده است. عملکرد دوربین گامای جدید به روش مونت کارلو شبیه سازی و مورد تجزیه و تحلیل قرار گرفته است.

INTRODUCTION

Hydrogenated amorphous silicon (a-Si:H) films can be coated on a variety of substrate materials using various deposition techniques. It is commonly produced by the decomposition of silane gas in plasma enhanced chemical vapor deposition (PE-CVD) chamber. The usefulness of this material in electronic applications was recognized in 1976, when the possibility of doping of this material, and therefore, making p-n junctions was reported[1]. Since then it has been the most widely used material for solar cells and has also been used as thin film transistor (TFT) switches in fax machine heads, flat monitor screens, and electrocopying machines [2]. Radiation detection applications of a-Si: H for X and γ rays, neutrons, and charged particles are established [3,4,5]. As a detector for nuclear radiation or light. (Solar cell) a-Si:H material is used in the form of reverse biased n-i-p diodes. The intrinsic layer is the radiation sensitive part and in photodiodes, it needs to be made 0.5-1 μm thick. The n and p layers are produced by addition of small concentrations of phosphine (PH_3) and diborane (B_2H_6) to the main process gas (silane), and are normally made about 20-30 *nm* thick. The choice of substrate depends on the application. For radiation detectors, Corning 7059 glass or Kapton can be used. Metallic contacts for electrodes are usually vacuum-coated or sputtered thin chromium layers or, light transparent indium tin oxide (ITO) films. For X and γ rays detection, a layer of a proper phosphor material is required to convert the incident radiation to visible light, which produces electron hole pairs in the intrinsic layer of the a-Si:H photodiode. Development of large area X and γ ray imagers and their associated electronic readouts has been reported [6,7]. Although certain electronic characteristics of a-Si:H are inferior to crystal silicon, the possibility of making low cost large area devices, as well as its inherent radiation hardness makes it advantageous in many imaging applications. Recently we have shown that certain electronic properties of a-Si:H are improved by hydrogen dilution of the process gas[8,9].

In this paper we first review applications of a-Si:H photodiodes in medical radiography and nuclear medicine. Then present our scheme for enhancing spatial resolution of CsI(Tl) scintillator layers, and finally discuss simulation results on the performance of our prototype a-Si:H based gamma camera.

NEW TRENDS IN MEDICAL IMAGING DETECTORS

Various forms of digital radiography, using the conventional radiographic films or image intensifier tubes, have been utilized for certain medical applications over the last two decades. During the last few years the development of large area and high density a-Si:H pixel arrays has provided a potential for real time imaging that may soon be able to completely supplant X-ray screen films. Although the newly developed 1536×1920 pixels a-Si:H sensor arrays with a pixel pitch of 127 μm [7] do not yet offer the spatial resolution comparable to radiographic films, it prove to be superior to the current real time imaging technologies in many aspects. The existing system used in fluoroscopy utilizes image intensifier tubes with CsI(Na) X-ray sensitive layers to form an image on a small solid state detector such as a charged coupled device (CCD). Image intensifier tubes are very reliable, but they have some disadvantages due to their bulk high cost and low resolution resulting from imperfect electron optics and loss of sharpness in optical couplings. In the real time imaging of megavoltage photon treatment beams (^{60}Co, or 3 to 50 MV X-ray) used in cancer therapy, demand for resolution is modest, ~1 lp/mm, and therefore a pixel pitch of ~500 μm is sufficient. For diagnostic X-ray imaging (~25 to 150 KVp), a resolution of 4-5 lp/mm is required to compete with most routine radiographic and fluoroscopic equaiment. A-Si:H based two dimensional arrays with pixel pitch of 127 μm reported in Reference 7 nearly provides this resolution. Considering the current trend of exponential increase in the pixel counts per imaging array with time [6], the outlook for the future of this technology is even brighter. Other performance characteristics of a-Si:H based imagers are signal to noise ratio linearity readout speed and image lag. The latter two are important in X-ray fluoroscopy and are addressed in Reference 10. It has been shown that the high resolution a-Si:H arrays are capable of providing fluoroscopic images at rates of at least 30 frames per second. For diagnostic medical X-ray assuming an exposure of $0.1R$, approximately 10^{12} visible $photons/cm^2$ are created in the scintillator, which results in a large signal charge of ~10^4 fC for a $100 \times 100 \mu m^2$ pixel, providing an excellent dynamic range for this kind of application. The response linearity of a-Si:H imaging pixels at a reverse bias ~2.5 volts is better than 1% for more than 85% of the full signal range [11]. The application of the a-Si:H arrays for tomographic imaging has also been investigated and their adequacy for acquiring X-ray transmission scan for attenuation correction in PET and SPECT imaging is reported[12].

The new generation of X-ray imagers consists of two major components, (a) phosphor screens, and (b) photosensitive detector arrays. In a phosphor material electron-hole paris produced by interaction of incoming radiation recombine to generate visible photons. For X-ray conversion several scintillator screens such as, Lanex (Kodak) and Chronex (Dupont) are commercially available. Better light collimations can be obtained by fiber optic plates with rare earth scintillators such as, terbium or cerium, with fiber sizes as small as 20 μm [13]. A more appropriate scintillator for coupling with a-Si:H photo-diodes is CsI (Tl). Below, we will discuss vacuum evaporated CsI(Tl) scintillator layers with columnar structure developed at Lawrence Berkeley National Laboratory.

Semiconductor photo sensitive arrays such as CCD and silicon p-n junction photo-diode arrays (PDA) are widely used today. A major disadvantage of these devices is the small array size of $3 \times 5 cm^2$ which restricts their direct use for most medical radiation imaging applications [4]. A-Si:H sensor arrays are now considered as advantageous alternatives for medical imaging applications. In the following some insight into the structure and operation of these arrays will be given.

A. A-Si:H Imaging Arrays

Amorphous silicon photodiodes can be integrated with their readout electronics on large area substrates to form pixel arrays with two dimensional position sensitivity. In these arrays, in order to achieve a high fill factor (radiation sensitive fraction of the total pixel area). Each pixel photodiode is deposited on the top of its associated TFT switch or amplifier. With today's technology, $30 \times 30 cm^2$ arrays with pixel sizes of $100 \times 100 \mu m^2$ are achievable and arrays as large as $60 \times 60\ cm^2$ are predicted to be available by the end of the decade[6].

Depending on the mode of operation two different schemes for signal readout are applicable (a) image scanning, and (b) position detection readout [15]. In the scanning mode, (Figure 1a) signal charge is stored on the pixel capacitance during the off period of the TFT switch. The stored charge is later read out by turning the TFT on, so that the signal charge can be transferred, through a data line to a charge sensitive amplifier. All pixles in a row have a common gate line, and all pixels in a column share a single data line. Scanning is performed by sending sequential pulses

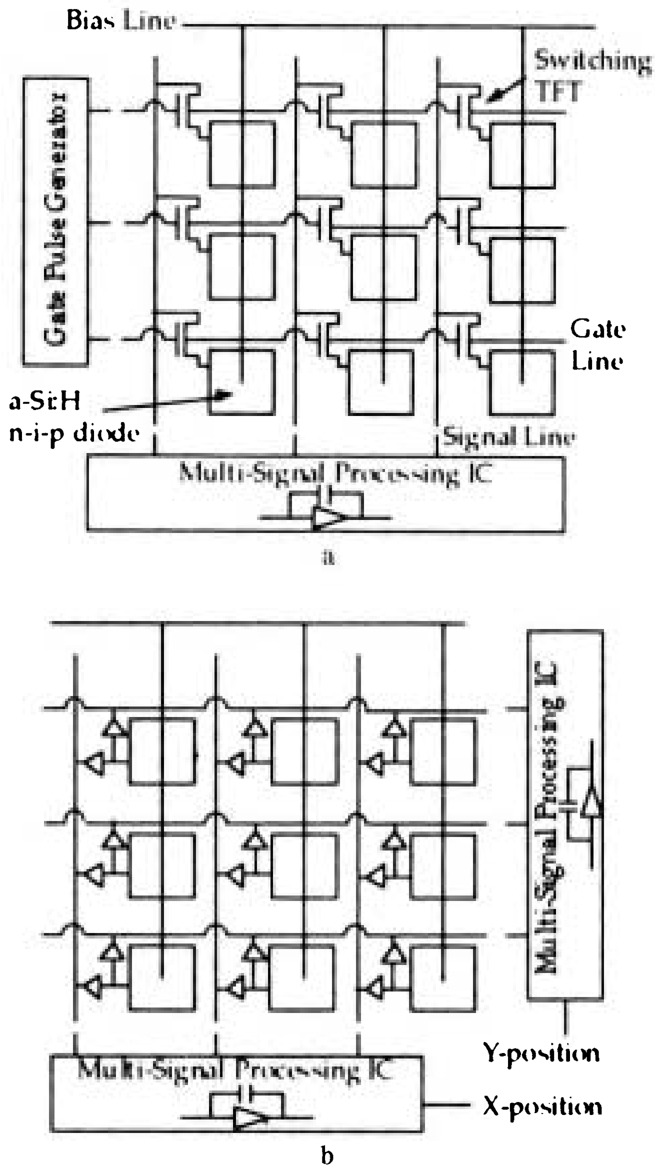

Figure 1. Schematic diagram of a-Si:H pixel array with readout electronics, (a) Image scanning readout, (b) position detecting readout for event-by-event collection mode.

to the gate lines, and after each pulse, reading output from the amplifiers connected to the data lines successively. In the position detection readout scheme (Figure 1b), each pixel has its own charge sensitive amplifier which sends output to both an X and Y data line. Each incoming photon on the array may produce signal charges in several adjacent pixels. The X and Y lines producing the largest signal identify the positon of the incident photon.

B. High Resolution CsI(Tl) Phosphor Layers

CsI(Tl) is known to be one of the most efficient scintillators for charged particles and for X-radiation and can emit more than 60,000 *photons/MeV* absorbed energy under optimal conditions[16]. As shown in Figure 2, the peak emission of this scintillator is about 580*nm*, which coincides very well with the peak collection efficienty of a-Si:H. However, for a photo-diode array coupled with a CsI(Tl) converter layer the spatial resolution will be restricted by the diffusion of photo-luminescent photons within the scintillator layer, if proper collimation of light does not occur. We have developed a new approach for the fabrication of CsI(Tl) layers which results in formation of a sequence of columns of regular controlled size (diameter) perpendicular to the substrate (detector) [17, 18]. This structure provides the scintillator with a light collimation which improves radiation detection resolution. Formation of the columns are enhanced by evaporating the scintillator on a patterned substrate. The substrate shown in Figure 3 is a thin (10-15μm) polyimide coated on Si wafer and then patterned using standard photo lithographic techniques. The CsI(Tl) layer is then vacuum evaporated using CsI and $TlCl_2$ powders in two separate boats and operated at different temperatures in order to control the Tl to CsI composition ratio [18]. For an optimum light yield a minimum Tl activator molecular concentration of 0.2% is required. Figure 4 shows SEM (scanning electron microscope) micrographs of CsI(Tl) layers deposited on patterned substrates, (a) before and (b) after annealing at 500°C. As it can be seen the annealing reduces the spreading of columns near the top and also widens the gap between columns hence further enhancing the light collimation of the structure. In Figure 5 we show the modulation transfer function (MTF) for (a) Lanex fast screen, (b) non-structured CSI (Tl) crystal 220 μm thick, (c) structured CsI (Tl) layer 220 μm thick, (d) Lanex fine screen 75μm thick, and (e) structured CsI(Tl) layer 75 μm thick [18]. It can be seen that the structured CsI(Tl) layers (c and

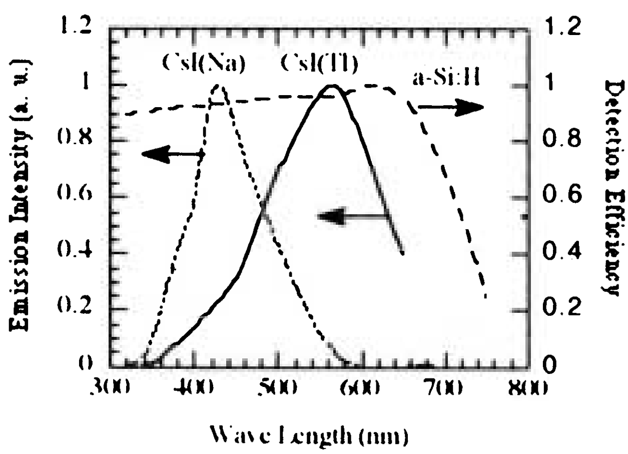

Figure 2. Emission spectra of CsI(Tl), CsI(Na), and a-Si:H response.

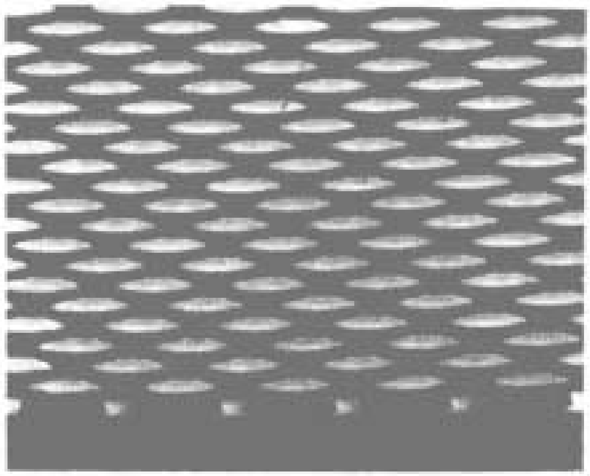

Figure 3. SEM of a patterned substrate used for CsI (Tl) coating.

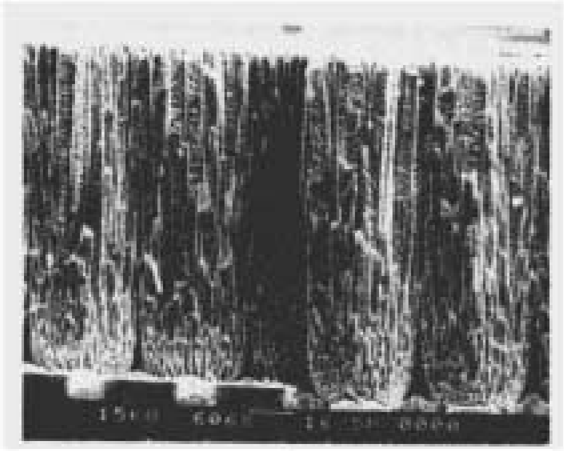

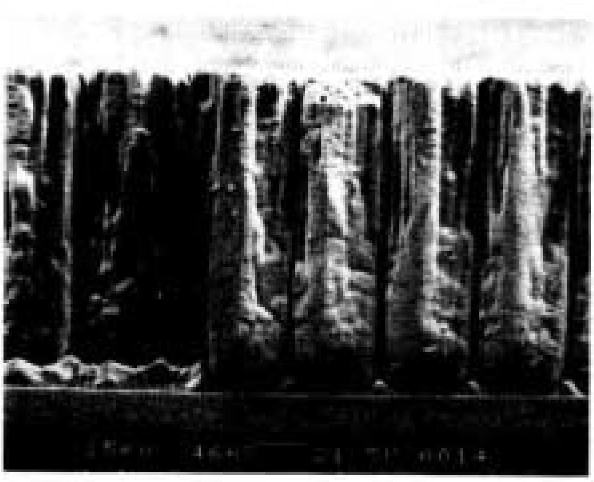

b

Figure 4. SEM of CsI (Tl) layers deposited on patterned substrates. (a) columnar structure before annealing, (b) after annealing at 500°C.

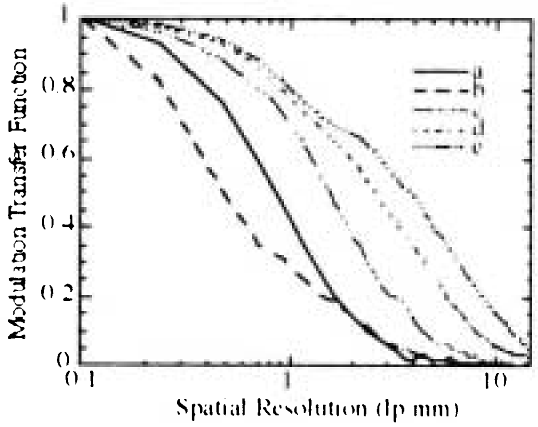

Figure 5. Modulation Transfer functions for **(a)** Lanex fast screen, **(b)** non-structured CsI(Tl) crystal 200μm thick, **(c)** structured CsI(Tl) layer 220 μm thick, **(d)** Lanex fine screen 75 μm thick, **(e)** structured CsI (Tl) layer 75μm thick.

e) show a substantial improvement over those of the Lanex screens and non-structured CsI(Tl) layer. The spatial resolution at 10% level for curve (e) is ~ 12 *lp/mm*. As a comparison a structured CsI(Tl) layer ~110μm thick produces more than twice as much light as a Kodak Lanex fine screen with an equivalent resoultion does. The evaporated CsI(Tl) layer is more resistant to radiation damage than a crystal; its light output is only reduced by a factor of 2 after exposure to 10^4 Gy of Co-60 γrays. More detailed measurement and analysis of the structured CsI(Tl) scintillator layers may be found in References 17,18. The results of these studies indicate that such a scintillator layer is a good candidate for coupling with an a-Si:H pixel array to be used in medical imaging.

NUCLEAR MEDICINE IMAGERS

The conventional device currently used in nuclear medicine is an improved version of the so-called "Anger Camera"[19], which consists of a collimator, NaI scintillator photo-multiplier tubes (PMT), and position sensing circuitry. The resolution is limited by the thickness requirement of the scintillator and is normally not better than 3*mm* FWHM. A gamma camera based on a-Si:H pixel arrays and CsI(Tl) scintillator would have several advantages such as higher resolution, compactness, portability and lower cost.

A. A-Si:H based Gamma Camera

In nuclear medicine, the requirements of the imaging devices are different from diagnostic and MV X-ray treatment imaging. In this application, the most widely used source is ^{99m}Tc and during the 3 minute data acquisition by the camera not more than ~10^6 γ rays is acquired from 20×20 mm^2 area of the body. This results in a 140*keV* gamma ray fluence of ~2500 photons cm^2, and produces about 10^7 visible photons cm^2 in scintillator and a similar number of electron-hole pairs in the photodiode. Therefore, a 3 minute stored signal charge of ~10 fC per mm^2 for the sensitive area of a pixel is expected, which is well above the noise. The problem with such a long integration time is the lack of charge retention due to leakage through the finite resistance of the photodiode and the OFF-state of the TFT switch. Based on a practical integration time of 20 sec.[20] with a conventional a-Si:H pixel and TFT switch, several succesive readouts are required. However, we have developed a new long term charge storage photodetector[21], which integrates the pixel diode with an external capacitance. This capacitance effectively blocks the leakage current and makes it possible to integrate the charge for 3 *min* provided that the thermal generated current in the diode is kept low by operating at low temperature[20].

B. Gamma Camera Monte Carlo Simulation

The performance of an a-Si:H based gamma camera was evaluated by a Monte Carlo simulation method. For the simulation, ^{99m}Tc (E_γ = 140 *KeV*) and ^{20}Tl (E_γ= 70 *keV*) sources were used. Here we briefly describe some of the results because more details on the assumptions and results are given in Reference 22. The analysis shows that for the 70*KeV* source, a 2*mm* thickness of CsI (Tl) is sufficient to absorb 99% of the γ-rays and for this thickness of scintillator, the spatial resolution of the camera composed of an array of 1×1 mm^2 pixels without any collimation is about 2*mm*. However, for the 140 *KeV* source a CsI (Tl), thickness of 5*mm* is required and with the same array the resolution is ~2.2*mm*. A water phantom with three different regions as shown in Figure 6 was used for the simulation. The parameters

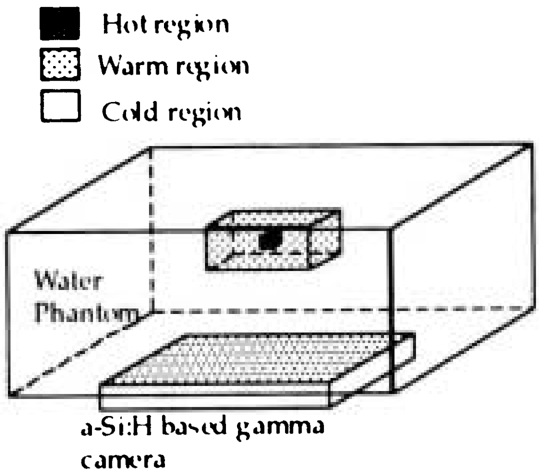

Figure 6. The geometry of the water phantom with hot, warm and cold sources.

of the water phantom and the γ-camera are given in Table 1. In Figure 7 we show the point spread function (PSF) of the camera for point sources in the water phantom at 5 and 10 *cm* distances from the collimator surface and γ-ray energies of 70 and 140*keV*. For this part of the simulation warm and hot regions were removed. The peak in the PSF corresponds to the response of the camera. Whereas the exponential tails are due to the scattering in the phantom. As it is seen, the slope of the tails depends

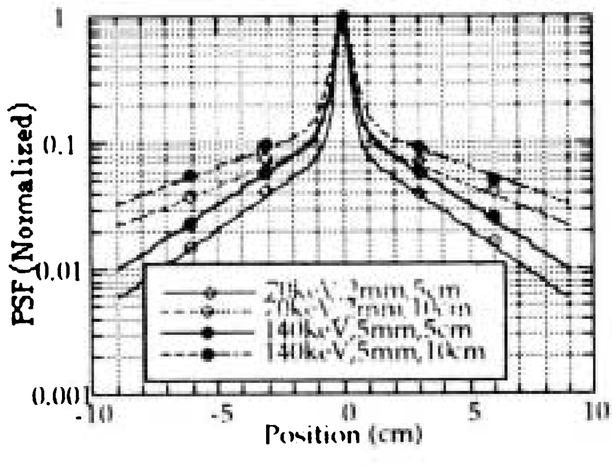

Figure 7. PSF from a point source in the water phantom with different g energies (70 *KeV* and 140 *Kev*) Source depths (5 and 10 cm), and scintillator thicknesses (2 and 5*mm*).

TABLE 1. Parameters of the Water Phantom and the Detector.

Cold region	size = $30 \times 30 \times 15 cm^3$, 0 kBq ml
Warm region	size = $30 \times 4 \times 4 cm^3$, 83.5 kBq ml
Hot region	size = $8 \times 8 \times 8 cm^3$, 918.5 kBq ml
γsource	^{99m}Tc or ^{201}Tl
Distance	7cm between phantom and collimator
Scintillator	2mm or 5mm thick CsI(Tl)
Detector area	$12.8 \times 12.8 cm^2$
No. of pixels	128×128 with pixel size of 1 x m²

on the source depth in the phantom and increases with the source-collimator distance. This kind of scattering is also observed in conventional gamma cameras and can be reduced by using an energy window discrimination. In a-Si:H gamma camera (integration mode) such a discrimination is not possible. However , the blurring which occurrs in the image due to this scattering can be drastically reduced by using an appropriate calculational filter. Figure 8 shows, (a) the true image of the phantom, (b) the simulated Scintigram image with a-Si:H based gamma camera, and (c) the simulated image with a conventional camera. The same source (^{99m}Tc) and collimation were used for both cameras, and for the conventional camera the parameters of a ZLC75 Siemens camera was used. The blurring effect due to scattering can be restored by applying a Wiener filter[23]. Before restoration a Gaussian pixel noise of 2fC was added to the image of Figure 8b. The result was used as the input image in the restoration process. The restored image is shown in Figure 9. In Figure 10 we show the profiles of the images in X-direction. As it can be seen from these figure, with restoration the quality of the image from a-Si:H based gamma camera is even better than that of the conventional camera.

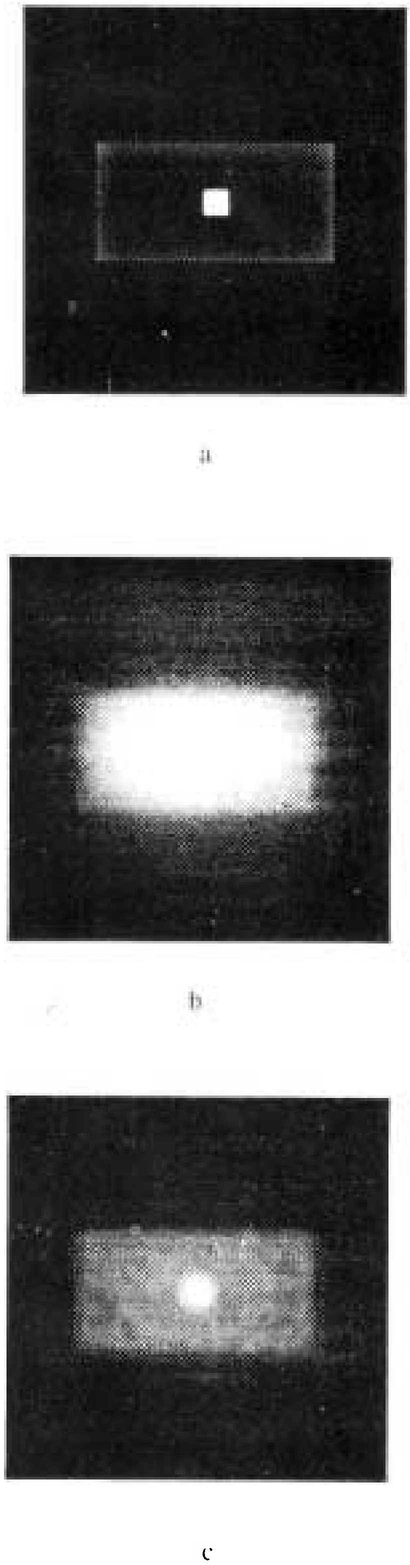

Figure 8. Images from simulationF: (a) true object, (b) simulated image with a Si:H based gamma camera, and (c) simualted image with conventional camera.

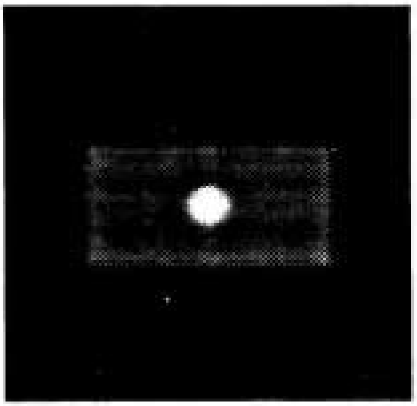

Figure 9. Restored image using Wiener filter. Image of Figure 8 (b) with added electronic noise was used as the input image.

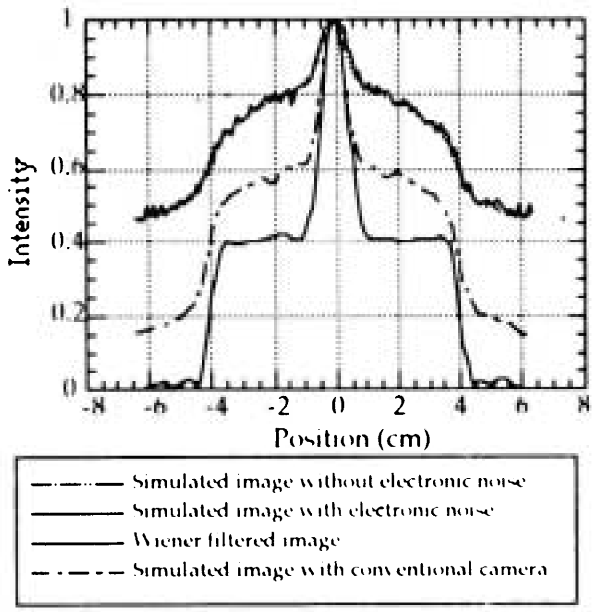

Figure 10. Profile of images in x-direction. Intensities are normalized to the maximum.

CONCLUSION

Recent advancements in the development of a-Si:H sensor arrays and their integration with associated electronic readouts have made it possible to compete with currently used technology for most applications in the medical imaging. The largest reported array with 3×10^6 pixels and pixel pitch of $127\mu m$ has good response linearity and high signal to noise ratio. It can be operated under X-ray radiographic or fluoroscopic conditions (30 frames per sec). We have developed a high resolution CsI(Tl) scintillator layer with columnar structures to enhance light collimation. These layers can be coupled with a-Si:H arrays with high efficiency by directly evaporating them on the arrays. The structured $110\mu m$ thick CsI(Tl) layers have spatial resolution of ~12 *lp/mm*. We have also evaluated the performance of an a-Si:H based gamma camera by Monte Carlo simulation. After restoration of the images by Wiener filter the quality of the simulated image from the camera is better than that of the conventional Anger camera.

REFERENCES

1. W. E. Spear and P. G. LeComber, "Substitutional Doping of Amorphous Silicon," *Solid State Comm.*, Vol. 17, (1975), 1193.
2. S. Kaneko and F. Okumura, "Amorphous Semiconductor Technologies and Devices," ed. Y. Hamakawa, OHMSA, (1987), 297-330.
3. V. Perez-Mendez, "Amorphous and Microcrystalline Semiconductor Devices," ed. J. Kanieki, Artech House, Boston, (1991), 297-330.
4. A. Mireshghi, G. Cho, J. Drewery, T. Jing, S. n. Kaplan, V. Perez-Mendez and D. Wildemuth, "Hydrogencued Amorphous Silicon Position Sensitive Neutron Detectors," IEEE Trans. Nuc. Sci. NS-39, No. 4, (1992), 635-640.
5. B. Equer and A. Karar, "Effect of Priary Ionization in Amorphous Silicon Detectors," *Nucl. Instrum. & Methods* A271, (1988), 571.
6. L. E. Antonuk, J. Boudry, Y. El-Mohri, W. Huang, J. Siewerdsen and J. Yorkston, "A High Resolution High Frame Rate Flat Panel TFT Array for Digital X-ray Imaging", SPIE: *Physics of Medical Imaging*, Vol. 2163, (1994), 118-128.
7. L. E. Antonuk, Y. J. Yorkston, W. Huang, J. Boudry, J.

Yorkston, E. J. Morton and R. A. Street, "Large Area Flat Panel a-Si:H Arrays for X-ray Imaging," SPH: *Physics of Medical Imaging*, Vol. 1896, (1993).

8. A. Mireshghi, W. S. Hong, J. Drewery, T. Jing, S. N. Kaplan, H. K. Lee and V. Perez-Mendez. "Improved Electrical and Transport Characteristics of Amorphous Silicon by Enriching with Microcrystalline Silicon," Res. Soc. Symp. Proc., 336, (1994), 377-382.
9. A. Mireshghi, W. S. Hong, J. Drewery, T. Jing, H. Lee. S. N. Kaplan and V. Perez- Mendez, "Improved Electronic Transport Characteristics of Amorphous Silicon by Hydrogen Dilution of Silane," *Japan. J. Appl. Phys. Partl.*, Vol. 34, No. 6A, (1995), 3012.
10. L. E. Antonuk, J. Yorkston. W. Huang, J. Siewerdsen and R. A. Street, "Considerations for High Frame Rate Operation of Two Dimentional a-Si:H Imaging Arrays." Mal. Res. Soc. Symp. Proc. 297, (1993), 945-950
11. J. Yorkston, L. E. Antonuk, W Huang and R. A. Steet, "Photoresponse Linearity of a-Si:H Imaging Pixels," Mat. Res. Soc. Symp. Proc. 297, (1993), 951-956.
12. N. H. Clinthorne. "Are Hydrogenated Amorphous Silicon Arrays Usable for Tomographic Imaging, ":IEEE Trans. Nucl. Sci. 41, (1993), 1692-1696.
13. E. Ellin: "Advanced Imaging," Scanteh Corp, (1988), 28-32.
14. M. G. Fedotov, E. A. Kuper and V. E. Panchenko, *Nucl. Instr. and Meth.*, Vol. 308, No. 10 (1991), 367-371.
15. G. Cho, J. S. Drewery, W. S. Hong, T. Jing, S. N. Kaplan, H. K. Lee, A. Mireshghi, V. Perez-Mendez and D. Wildermuth," A Measurement of the Light Yield of Common Inorganic Scintillators," *IEEE Trans. Nucl. Sci.*, NS-40, No. 4, (1993), 323-327.
16. I. Hall, E. Lorenz, G. Mageras, "A Measurement of the Light Yield of Common Inorganic Scintillators," *IEEE Trans. Nucl. Sci.*, NS-35, No. 1, (1988), 105-109.
17. T. Jing, G. Cho, J. Drewery, L. Fujieda, S. N. Kaplan, A. Mireshghi, V. Perez-Mendez and D. Wildermuth, "Enhanced Colummar Structure in CsI Layers by Substrate Patterning, "*IEEE Trans Nucl. Sci*, NS-39, No. 5, (1992), 1195-1198.
18. T. Jing, C. A. Godman, G. Cho, J. Drewery, W. S. Hong, H. Lee, S. N. Kaplan, A. Mireshghi, V. Perez-Mendez and D. Wildrmuth, "Improvement in Detective Quantum Efficiency of Structured CsI Layers, "*IEEE Nucl. Sci. Symp. Conf. Rec.* Vol. 3 (1993) 1878-1882.
19. W. R. Hendee, "Medical Radiation Physics, "2nd ed., Year Book Medical Publishers, (1979), 271.
20. I. Fujieda, S. Nelson, R. A. Street and R. I. Weisfield, "Radiation Imaging with 2-D a-Si:H sensor Arrays," *IEEE Trans. Nucl. Sci.* NS-39, (1992), 1056-1062.
21. H. Lee, G. Cho, J. S. Drewery, W. S. Hong, T. Jing, S. N. Kaplan, A. Mireshghi, V. Perez-Mendez and D. Wildermuth, "New A-Si:H Photodetectors for Long Term Charge Storage," Mat. Res. Soc. Symp. Proc., Vol. 297, (1993), 1023-1028.
22. H. K. Lee, "Application of A-Si:H Radiation Detectors in Medical Imaging, "Ph. D. Thesis, University of California, Berkeley, (1995).
23. T. R. Miller and K. S. Sampathkumaran, "Design and Application of Finite Impulse Response Digital Filters," *Eur. J. Nucl. Med.*, 7, 22, (1982).